Article published online: 2022-03-30

Review Article

^{18}F-fluorodeoxyglucose positron emission tomography/computed tomography imaging review of benign lesions of the thorax

ABSTRACT

2-deoxy-2-(Fluorine-18) fluoro-D-glucose (^{18}F-FDG) positron emission tomography/computed tomography (PET/CT) has been used exclusively to diagnose malignancies. However, increased ^{18}F-FDG uptake is not always limited to malignant lesions. This imaging review demonstrates the physiological ^{18}F-FDG uptake of normal structures in the thorax and illustrates many benign pathological lesions with standardized uptake value >2.5. These various conditions can be broadly categorized into three groups: infective lesions, active granulomatous diseases such as sarcoidosis, noninfectious/inflammatory, or proliferative conditions such as radiation pneumonitis, postlung transplant lymphoproliferative disorders, occupational pleuropulmonary complications, and postsurgical conditions, all of which can demonstrate varying degrees of ^{18}F-FDG uptake on PET/CT based upon the degree of inflammatory activity. Familiarity of false-positive findings improves the PET/CT evaluation accuracy of benign lesions of the thorax. Radiation exposure and surgical history correlation along with imaging cross check evaluation of radiographs and magnetic resonance images for the anatomic location remains the mainstay of PET/CT characterization of positive findings.

Keywords: 2-deoxy-2-(Fluorine-18) fluoro-D-glucose positron emission tomography/computed tomography, active granulomatous diseases, benign lesions of the thorax, infective lesions, inflammatory or proliferative conditions

INTRODUCTION

Positron emission tomography/computed tomography (PET/CT) imaging with 2-deoxy-2-(Fluorine-18) fluoro-D-glucose (^{18}F-FDG) is a combined functional and anatomic imaging modality widely used to evaluate, stage, and monitor malignancy.[1] The abnormal areas of ^{18}F-FDG accumulation are identified by qualitatively comparing the tracer uptake with normal background activity. However, ^{18}F-FDG affinity is not malignancy specific and during the PET/CT oncologic evaluation, imagers may encounter incidental and/or co-existing ^{18}F-FDG avid findings, which are not related to the investigated malignant processes. This may lead to false-positive results and incorrect diagnostic predicaments, which may significantly impact the care and welfare of patients. Accurate diagnosis can reduce unnecessary invasive procedures such as biopsy and thoracotomy in patients with benign disease,[2] and therefore, familiarity with the different causes of increased ^{18}F-FDG uptake in the thorax mimicking cancer is imperative. This imaging review encompasses inflammation, infection, physiologic variants, trauma, iatrogenic processes, posttherapeutic changes and benign

Reddy Ravikanth

Department of Radiology, St. John's Hospital, Kattappana, Kerala, India

Address for correspondence: Dr. Reddy Ravikanth, Department of Radiology, St. John's Hospital, Kattappana - 685 515, Kerala, India.
E-mail: ravikanthreddy06@gmail.com

Submitted: 20-Jun-2020, **Revised:** 20-Jun-2020, **Accepted:** 29-Jun-2020, **Published:** 07-Oct-2020

Access this article online	
Website: www.wjnm.org	Quick Response Code
DOI: 10.4103/wjnm.WJNM_85_20	

How to cite this article: Ravikanth R. ^{18}F-fluorodeoxyglucose positron emission tomography/ computed tomography imaging review of benign lesions of the thorax. World J Nucl Med 2021;20:7-16.

diseases of the lung parenchyma, pleura, and different components of the mediastinum and chest walls based on etiology for optimized diagnosis based on its thoracic location [Table 1].

PHYSIOLOGIC VARIANTS

Muscle tracer uptake is related to voluntary or involuntary exertion, increased insulin level, or postprocedural changes. Exertion up to 48 h before PET/CT imaging may result in muscle uptake.[3] Positive uptake features are mostly demonstrated in the head and neck, trunk, extremities, and diffusely throughout the body from different causes such as neck strain lying on stretcher, chewing gum, talking, finger tapping, cough, labored breathing, muscle spasms, jerking movements from seizure, and more. Familiarity with muscle uptake features (anatomic locations and symmetrical patterns) and knowledge of recent voluntary or involuntary exertion prior to PET/CT imaging are helpful to avoid false-positive diagnosis of cancer [Figure 1].

Brown adipose tissue is a well-known cause of false-positive uptake on PET/CT due to the hypermetabolic nature of the tissue.[4,5] Brown fat may be detected in 4%–5% of all PET/CT cases more frequently in women than in men.[6] The frequently encountered patterns of brown adipose tissue are bilateral and symmetrical at sites of CT-depicted fat tissue attenuation of sub-occipital, cervical, supraclavicular, axillary, paraspinal, and intercostal regions [Figure 2]. Intermittently, brown fat deposit may be at less common and asymmetrical locations potentially leading to an interpretation error, specifically along the sternum mimicking mammary lymph nodes.

Table 1: Diagnostic benign lesions of thorax with corresponding median SUV_{max} values

Diagnosis	Median SUV_{max} value
Inflammation	4.6
Brown adipose tissue	2.0
Cardiac uptake (right atrium/atrial appendage and left atrium, left atrial appendage)	4.2
Lipomatous hypertrophy of the inter-atrial septum	1.8
Inflammatory pseudotumor	2.5
IgG4-related sclerosing disease	8.4
Nodal sarcoidosis	5.9
Anthracosis	4.7
Thyroiditis	9.1
Pulmonary abscess	10.2
Pulmonary and nodal coccidiodomycosis	2.0
Postradiation changes	3.5
Radiation myocarditis	2.4
Talc pleurodesis-induced granulomatous reaction	11.0
Thorax postprocedural	5.1
Apical cardiac patch	2.7
Sternal fracture	5.5
Diffuse reactive marrow	2.8
Mediastinal schwannoma	4.2
Chest wall desmoid	1.7
Chest wall elastofibroma dorsi	3.6
Aneurysmal bone cyst	3.0

SUV_{max}: Maximum standardized uptake value

Myocardial metabolism may be from free fatty acid or glucose substrates depending on the fasting or nonfasting status of the patient. During oncologic imaging, the required patient's fasting forces the heart to use free fatty acid as substrate and should result in low and uniformed cardiac uptake features.[7] In real practice, the cardiac uptake patterns are variable even in serial PET/CT exams of the same patient. ^{18}F-FDG uptake by atrial appendages or atria is related to atrial fibrillation or overload physiology. The less frequent tracer uptake by ventricles or simultaneously to all chambers of the heart may be secondary to pressure overload or underlying valvular heart diseases.[8] Correlation with additional cardiac imaging (CT, echocardiography, and magnetic resonance imaging [MRI]) may be useful to distinguish benign cardiac uptake from metastatic tumor and mediastinal lymphadenopathy[9] [Figure 3].

Lipomatous hypertrophy of the interatrial septum (LHIS) is a benign fat accumulation in the interatrial septum with a prevalence of 2%–3%. CT at the level of the fossa ovalis shows a "dumb-bell" shape due to sparing of the fossa in 78% of patients with LHIS. LHIS demonstrates a greater mean standardized uptake value (SUV) on PET/CT when compared to chest wall fat.[10] This is due to the increased amount of

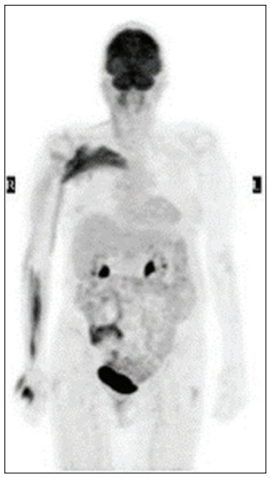

Figure 1: Whole body maximum intensity projection image demonstrating increased radiotracer uptake at the musculature of the right neck, right shoulder girdle predominantly at the pectoralis major and subscapularis muscles, and entire right upper extremity due to involuntary dyskinetic muscular exertion from recent seizure occurring <48 h before the positron emission tomography/computed tomography imaging

brown fat in LHIS, making it more metabolically active and thus ^{18}F-FDG avid. These features will help differentiate LHIS from malignant cardiac processes. Fat accumulation in the interatrial septum increases with patient's age and obesity.[11] The thicker and bulkier the fat infiltration of the interatrial septum, the more prominent ^{18}F-FDG uptake is seen. The diagnosis of LHIS rests on the fat attenuation characteristics demonstrated by the transmission CT [Figure 4].

Figure 2: Whole body positron emission tomography maximum intensity projection image demonstrating classic bilateral and symmetrical pattern of hypermetabolic brown adipose tissue at the sub-occipital, cervical, supraclavicular (arrows), axillary, and paraspinal regions

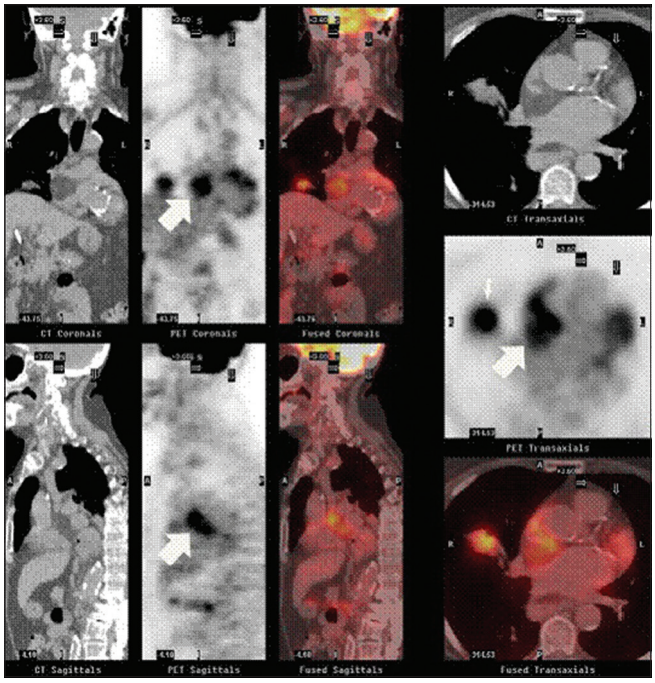

Figure 4: Composite positron emission tomography/computed tomography images demonstrating hypermetabolic lipomatous hypertrophy of the inter-atrial septum with corresponding tissue with adipose attenuation characteristics on transmission computed tomography (arrows). A right peri-hilar hypermetabolic lung malignancy is seen on axial images (small arrow)

INFLAMMATION

Lung inflammatory pseudotumor, also known as inflammatory myofibroblastic tumor, represents a spectrum of myofibroblastic proliferations containing a varying infiltrate of chronic inflammatory cells.[12] Radiographically, it is nonspecific featuring round/oval lung nodule or mass with possible speculations and variable degrees of contrast enhancement. Due to infiltrating inflammatory cell composition, it exhibits ^{18}F-FDG uptake simulating malignancy [Figure 5].

Resection of the lesion is the treatment of choice. However, nonsurgical treatments such as radiotherapy (RT) and steroids

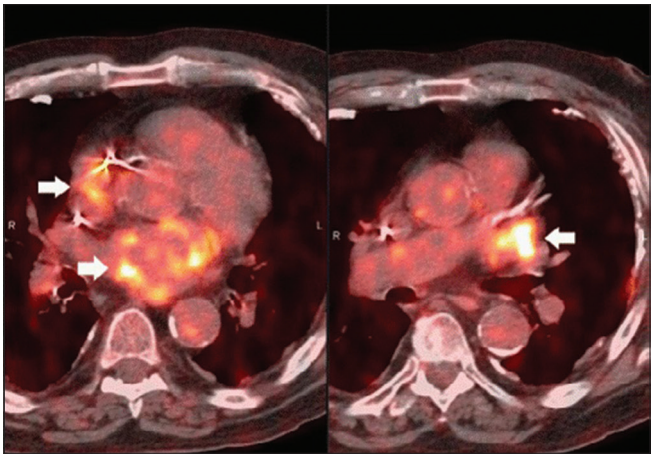

Figure 3: Composite positron emission tomography/computed tomography images demonstrating tracer uptake at the right atrium/atrial appendage and left atrium (arrows, left image) and left atrial appendage (arrow, right image), which could mimic hypermetabolic mediastinal nodal disease

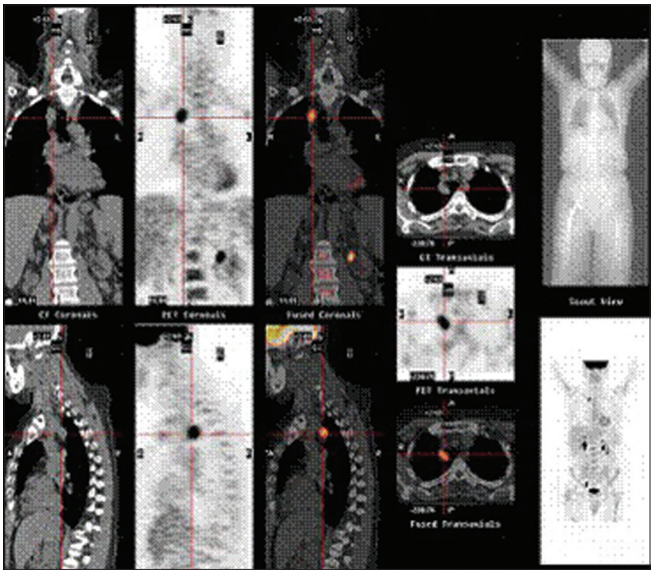

Figure 5: Composite positron emission tomography/computed tomography images demonstrating a spiculated right upper pulmonary lobe lesion with prominent tracer uptake (cross-hair) suspicious for lung malignancy. Histology of the resected lesion shows an inflammatory pseudotumor

have been employed in the setting of incomplete surgical resection, tumor recurrence, and patients being unfit for surgery. PET/CT can play a role in monitoring postradiation changes attempting to decrease surgical and further radiation treatments.[13] The definitive identification of lung inflammatory pseudotumor is histological.

Systemic IgG4-related sclerosing disease is characterized by lesions with lymphoplasmacytic infiltrative fibrosis. Also known as autoimmune pancreatitis due to the originally reported involvement of the pancreas, this disorder also features lesions of different organ systems of the body such as the orbits, salivary glands, thyroid, gallbladder, biliary ducts, retroperitoneum, aorta, kidneys, prostate, lymphatic system, airways and lungs [Figure 6]. Lung involvement is related to IgG4-positive plasma cell and lymphocyte infiltrating the parenchyma with immunohistochemically evident fibrous interstitial proliferation in the background. Correct diagnosis of this condition is crucial because steroid therapy can be curative. Unfortunately, malignancy cannot be differentiated from the imaging findings, and tissue sampling is necessary to confirm the diagnosis of IgG4-related lung disease.[14] Within the mediastinum, it can present with nonspecific bronchial wall thickening [Figure 7]. Recognizing additional areas of involvement, especially the bilateral and symmetrical orbital and salivary gland ^{18}F-FDG avid features, is helpful in differentiating the correct diagnosis from malignancy.

Sarcoidosis is a chronic systemic inflammatory disease of unknown origin involving preferentially lungs often with associated hilar and mediastinal adenopathy. Characteristic radiologic and PET/CT features of thoracic sarcoidosis are well recognized by clinicians and imagers and are actually used to follow the status of patients undergoing treatment.[15,16] Since the PET/CT features are frequently indistinguishable from other advanced neoplasms with mediastinal lymphadenopathy, histologic proof is typically necessary for the correct diagnosis of systemic inflammatory disease [Figure 8].

The false-positive PET/CT findings from reactive process to foreign material mimic nodal metastasis from lung malignancy. Mediastinal node staging with PET/CT in coal workers has been rendered insufficient due to the high false-positive rates given the presence of pneumoconiosis with positive predicted values as low as 66%.[17,18] Therefore, more invasive methods of nodal sampling are necessary in

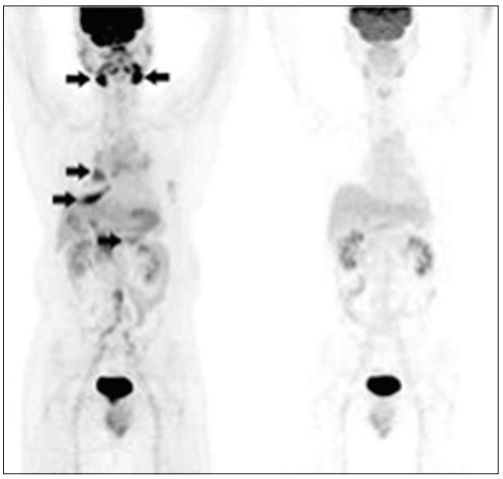

Figure 6: Whole body maximum intensity projection images of a patient with IgG4-related sclerosing disease before and after corticotherapy demonstrate resolution of tracer uptake at the bilateral salivary glands (top arrows), right hilar node, right lower pulmonary lobe (midlevel arrows) and pancreas (bottom arrow)

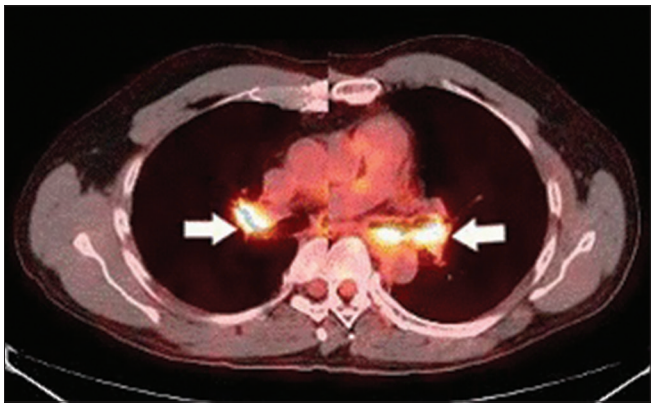

Figure 7: Composite positron emission tomography/computed tomography images demonstrating IgG4-related sclerosing lesions of bilateral bronchi with narrowing of the airways (arrows)

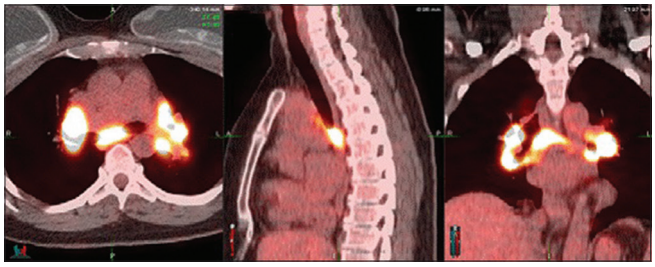

Figure 8: Composite positron emission tomography/computed tomography images demonstrating clustered hypermetabolic nodal disease in the mediastinum and bilateral hilar regions from sarcoidosis

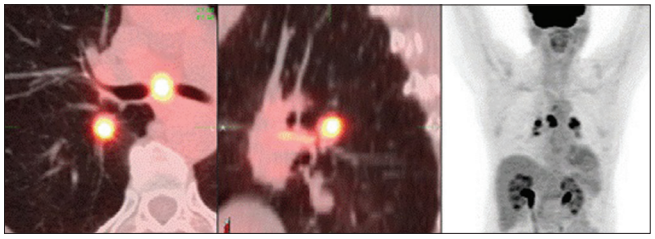

Figure 9: Composite positron emission tomography/computed tomography images in axial and coronal projections (left) and maximum intensity projection image (right) demonstrating hypermetabolic adenopathy in the subcarinal and bilateral hilar regions from histologically proven anthracosis

differentiating anthracosis from malignancy in patients with PET/CT positive lymph nodes and known pneumoconiosis exposure [Figure 9].

Thyroid uptake in PET/CT imaging poses a common conundrum among imagers. Diffuse uptake is typically associated with a benign pathology such as thyroiditis and focal nodular uptake may be related to hyperfunctioning nodules or malignancy.[19] Occasionally, a substernal thyroid is present and can present as a focal hypermetabolic mediastinal mass on PET/CT [Figure 10]. Three-dimensional PET/CT evaluation of the thoracic inlet is helpful to ascertain the origin of this potential lesion.

INFECTIONS

Thoracic infectious diseases may target the lung parenchyma, mediastinum, or chest wall. The high concentration of macrophages and inflammatory cells and consequently high ^{18}F-FDG avidity at sites of infection and abscess formation may mimic cancer especially at prior sites of resected/treated malignancy and the existence of cavitation reminiscent of malignant central necrosis [Figure 11].[20] Coccidioidomycosis is an endemic fungal disease of the arid and semi-arid regions of the North, Central, and South American continent and is secondary to inhalation of the arthroconidia form of Coccidioides immitis. This disease, primarily a regional public health concern, may be encountered worldwide due to the large population migration, and seasonal and recreational transit through the endemic areas. Risk factors are pregnancy, extreme stages of life, diabetes, corticosteroid use, immunocompromised health conditions and dark-skinned ethnics. Although the pulmonary manifestations of this infection vary and resemble those seen in mycobacterial infections,[21] the acute phase of the disease may present with nonspecific infectious findings such as infiltrates, consolidation, adenopathy, and pleural effusion[22] giving the appearance of a primary lung malignancy [Figure 12].

TRAUMA, IATROGENIC AND POSTPROCEDURAL CHANGES

Postradiation changes usually present with geographic/straight margin features involving organs and anatomic structures subjected to this procedure such as lungs and heart. Pulmonary parenchyma involvement exhibits the features of consolidation with fibrotic retraction with associated ^{18}F-FDG uptake. Patient's history and recognition of a radiation portal pattern are essential to avoid misdiagnosis [Figure 13]. Tracer uptake at the cardiac apex is related to the oblique/tangential radiation portals used for the treatment of left breast cancer. Radiation-induced cardiac toxicity using

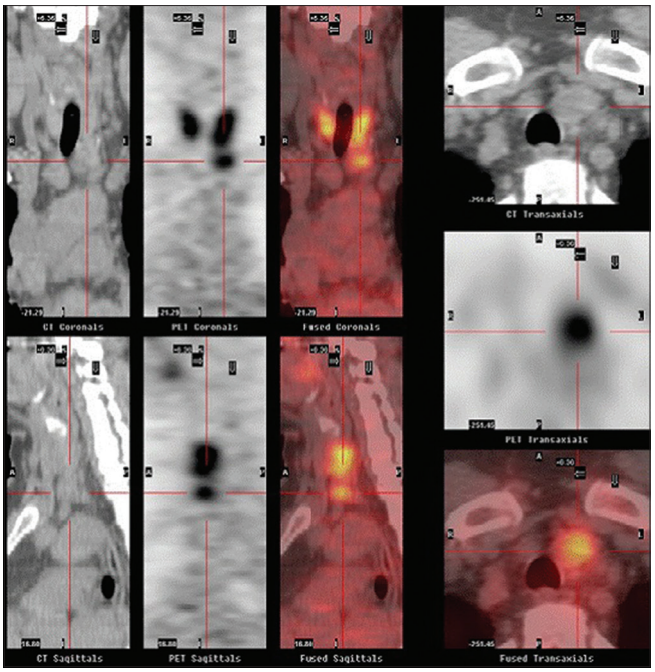

Figure 10: Composite positron emission tomography/computed tomography images demonstrating uptake features of thyroiditis with substernal component (crosshair). The diffuse pattern of F-18 FDG distribution in the thyroid gland is in favor of benign or inflammatory processes

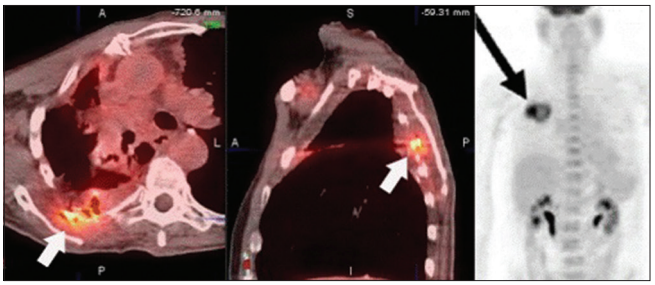

Figure 11: Composite positron emission tomography/computed tomography images (left) and maximum intensity projection image (right) of the right chest wall abscess and of right upper pulmonary lobe abscess with cavitation (arrow) in two different patients mimicking malignancy

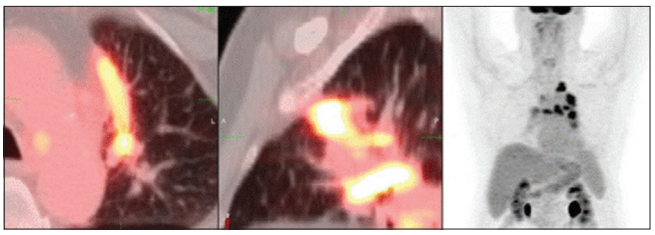

Figure 12: Composite positron emission tomography/computed tomography and maximum intensity projection images demonstrating coccidiodomycosis of the medial left lung and mediastinal and hilar nodes

myocardial imaging has demonstrated perfusion defects in 0%–70% of patients from 1 to 18 years post-RT for left-sided breast cancer. Radiation therapy may cause perfusion defects, wall motion abnormalities, and subtle changes in cardiac ejection fraction from 0.5 to 2 years post-RT. These perfusion

defects may persist from 3 to 6 years post-RT. Furthermore, new perfusion defects may appear 3–6 years posttreatment in patients who had initially normal cardiac SPECT scans after treatment.[23,24] It has been suggested that a radiation dose >35 Gy is required to result in increased ^{18}F-FDG activity [Figure 14]. Talc pleurodesis is a procedure to treat persistent pneumothorax or recurrent pleural effusion. The pleural deposits stimulate a chronic granulomatous reaction that may be ^{18}F-FDG avid and thus mimic tumor recurrence on PET/CT in patients treated for pulmonary or pleural malignancy [Figure 15]. The characteristic high CT attenuation of talc density from matched ^{18}F-FDG avid curvi-linear features helps to differentiate this entity from pleural tumors.[25] Hypermetabolic lung clot as focal tracer accumulation without corresponding CT abnormality has been associated with emboli; an inflammatory reaction of a preexisting vascular thrombus and iatrogenic from injection.[26] Occasionally a complicated tracer injection can induce an ^{18}F-FDG labeled

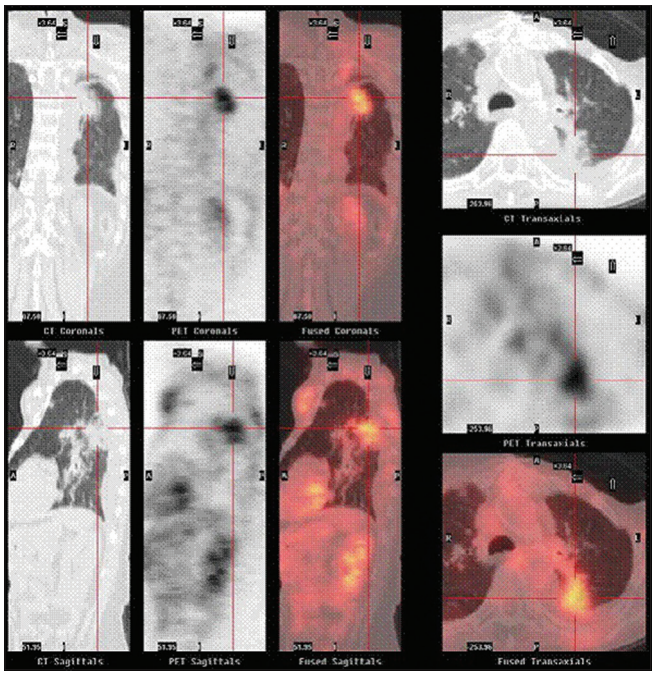

Figure 13: Composite positron emission tomography/computed tomography images demonstrating tracer uptake at the medial aspect of the left lung from postradiation changes (crosshair)

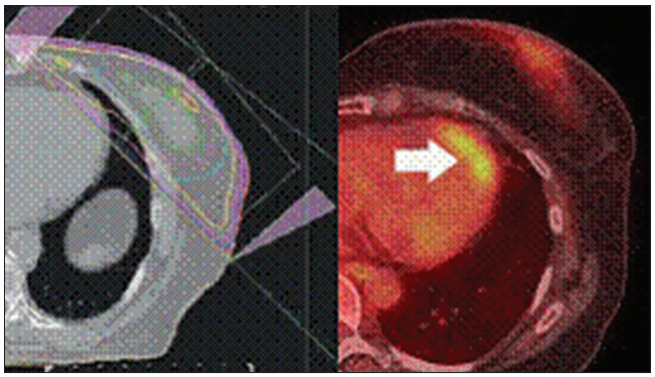

Figure 14: Composite image of the oblique radiation portal of the left breast cancer grazing the left ventricular apex (left) with resulting corresponding tracer uptake from radiation myocarditis (right, arrow)

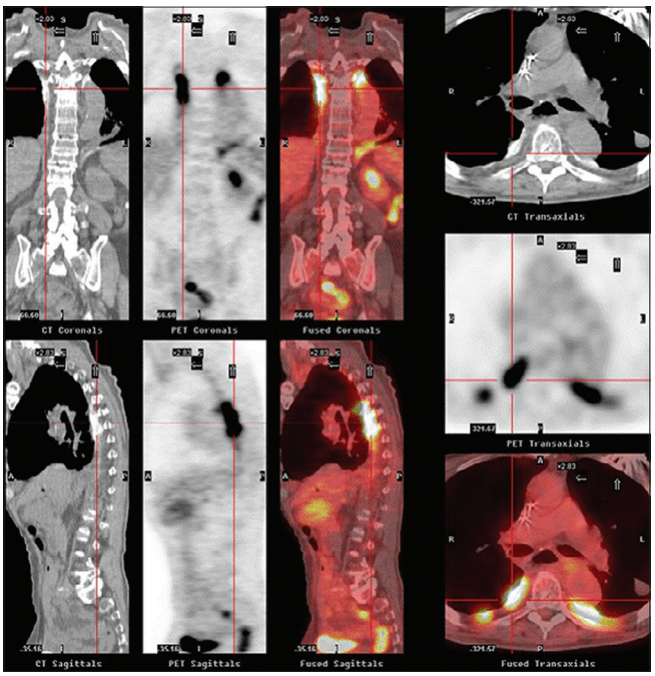

Figure 15: Composite positron emission tomography/computed tomography images demonstrating bilateral foci of curvilinear tracer uptake corresponding to sites of calcified pleura secondary to granulomatous reaction of talc pleurodesis (crosshair)

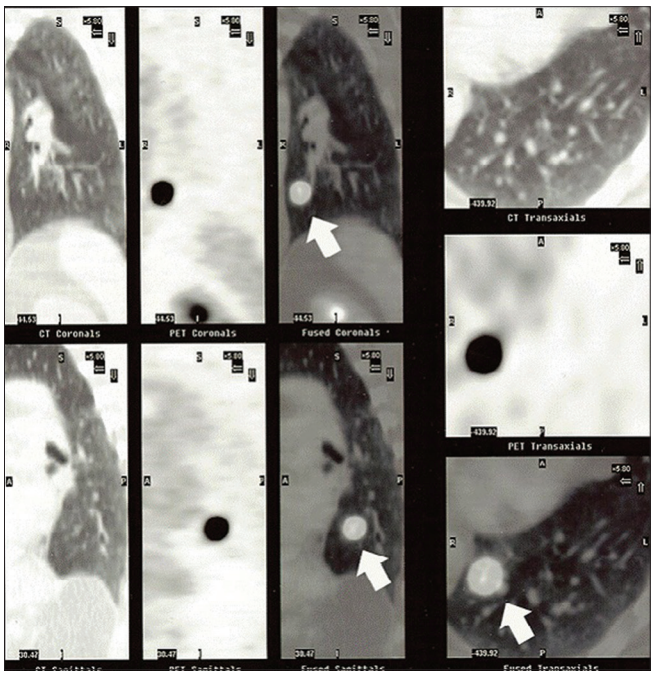

Figure 16: Composite positron emission tomography/computed tomography images demonstrating prominent nodular tracer uptake at the left lower pulmonary lobe without any corresponding soft tissue lesion on transmission computed tomography. The finding is related to complicated upper extremity tracer injection with hypermetabolic clot (arrow)

platelet aggregated clot to embolize causing a focus of tracer accumulation in a vascular branch without corresponding CT findings of visible thrombus [Figure 16]. Mediastinal and cardiac procedures or other recent instrumentation and invasive procedures induce local and regional concentration of inflammatory cells exhibiting increased tracer uptake on PET/CT imaging. Curvilinear and well-defined geometric features are strongly suggestive of sequela of man-made processes such as mediastinoscopy [Figure 17] and porcine pericardial patch repair [Figure 18]. Osseous injury whether from trauma (fracture) and iatrogenic (sternotomy) can lead to increased tracer accumulation on PET/CT due to build up and high turnover of inflammatory cells during active osseous repair and healing processes[27] [Figure 19]. The difference between SUV values of benign and malignant fractures has been shown to be statistically significant and therefore can aid in interpretation of abnormal uptake in the sternum.[28] A precise surgical/oncologic history is important when assessing the positive PET/CT osseous findings. Reactive bone marrow process the ^{18}F-FDG uptake in normal bone marrow is typically of low level. This uptake is increased

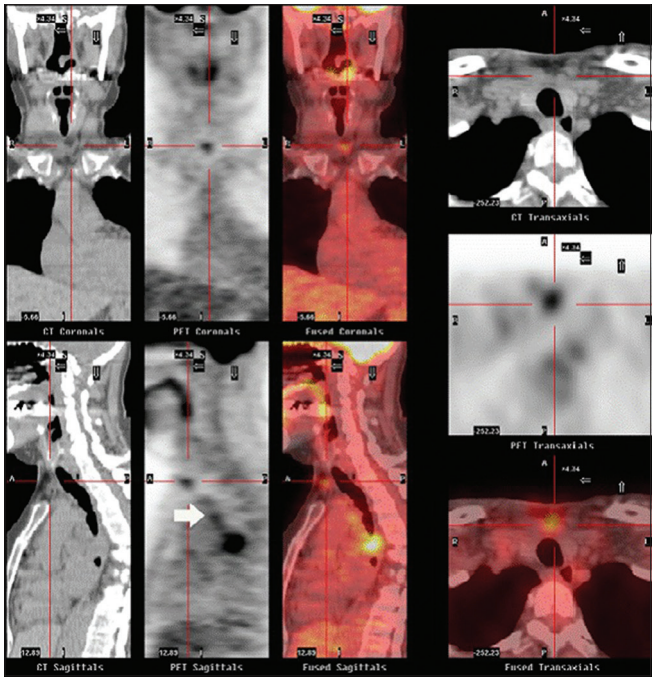

Figure 17: Composite positron emission tomography/computed tomography images demonstrating linear features of tracer uptake highlighting the tract of recent mediastinoscopy (crosshair and arrows)

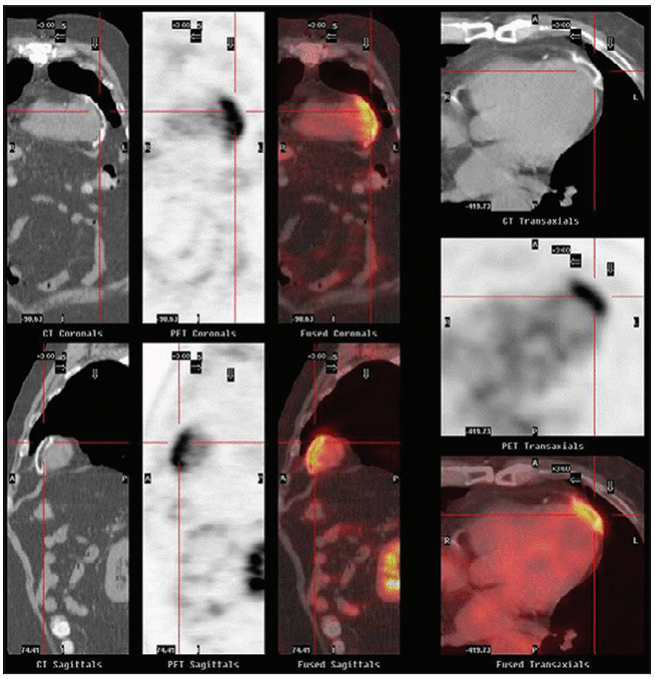

Figure 18: Composite positron emission tomography/computed tomography images demonstrating tracer uptake of the apical cardiac patch (crosshair)

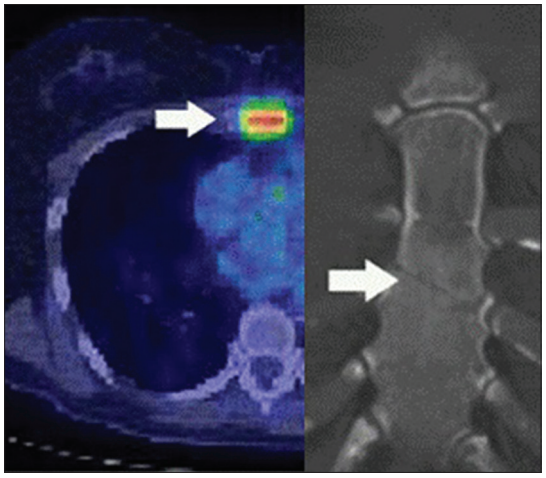

Figure 19: Composite images of axial positron emission tomography/computed tomography (left) and computed tomography coronal reconstruction of the sternum (right) demonstrating increased tracer uptake at the site of sternal fracture (arrows)

Figure 20: Whole body maximum intensity projection image demonstrating diffuse reactive marrow of the axial and appendicular skeleton secondary to chemotherapy and colony-stimulating factor medications

diffusely with a homogenous or heterogeneous manner in patients receiving chemotherapy and colony-stimulating factor medications [Figure 20]. The increased bone marrow activity may simulate malignant infiltration or interfere with the detection any underlying focal viable malignancy. Knowledge of the patient's therapeutic regimen and interval of time between the use colony-stimulating factors and the PET/CT imaging is important to accurate evaluation the bone marrow uptake.

BENIGN TUMORS

Schwannomas involve frequently spinal nerve roots, and nerves of the head and neck, and flexor surfaces of extremities. They are usually solitary in a patient population of third to fifth decades of life[29] with or without association with neurofibromatosis type 1. Their prominent ^{18}F-FDG uptake, not related to size or tumor proliferation rate characterized by the Ki-67 index may be linked to overexpression of glucose transporter proteins by the tumor cells.[30] Thoracic schwannomas may involve the mediastinum or chest wall [Figure 21]. PET/CT cannot distinguish schwannomas from malignant peripheral nerve sheath tumors or malignant nodal disease based solely on the uptake values. The diagnosis of schwannomas rests on histological identification. Fibromatosis is a group of benign soft tissue tumors with locally aggressive behavior characterized by proliferation of fibroblasts with mature collagen.[31] It is mostly associated with Gardner's syndrome. This syndrome is a rare autosomal dominant inherited disorder characterized by intestinal polyposis, bone and soft-tissue tumors, including osteomas, epidermal inclusion cysts, lipomas, fibromas, gastric and duodenal polyposis, frequently complicated by subsequent desmoid tumors of the mesenteric and abdominal/chest wall [Figure 22]. The PET/CT uptake features are probably related to high cellularity and mitotic activity of fibromatosis. Elastofibromas dorsi are benign soft tissue tumors characterized by fibroblastic proliferation and accumulation of abnormal elastic fibers with a reported prevalence on CT of 2% in the elderly population. These lesions are predominantly encountered in elderly women. They may be bilateral and asymmetrical in size in about 10% of all cases. MRI and CT show elongated soft tissue masses with combined characteristics of muscle and fat tissue. Elastofibromas are located between the ribs and serratus and latissimus dorsi musculature, deep to the inferior angle of the scapula. PET/CT shows mild to moderate degree of ^{18}F-FDG uptake. These cross-sectional and PET/CT features are helpful to avoid unnecessary biopsy during evaluation of primary and secondary malignancies[32] [Figure 23]. Other

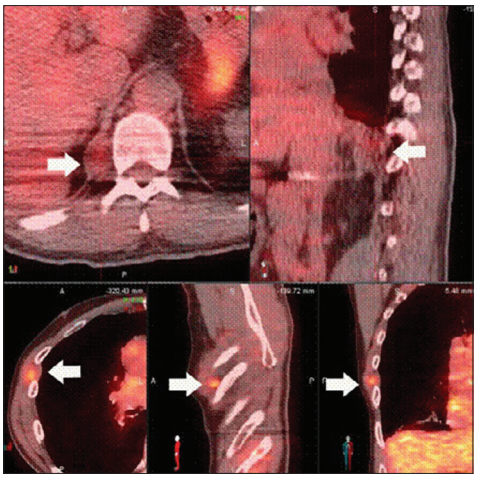

Figure 21: Composite positron emission tomography/computed tomography images demonstrating two benign schwannomas of the infero-posterior mediastinum at right retrocrural region (top row, arrows) and of the right chest wall at intercostal location (bottom row, arrows)

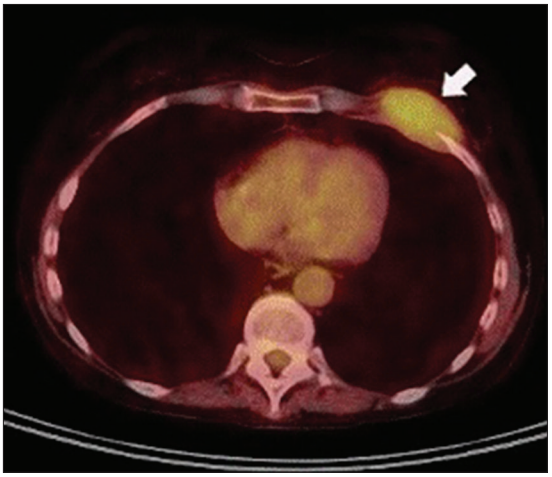

Figure 22: Axial positron emission tomography/computed tomography image of a patient with Gardner's syndrome demonstrating a hypermetabolic left anterior chest wall desmoid encasing an adjacent rib (arrow)

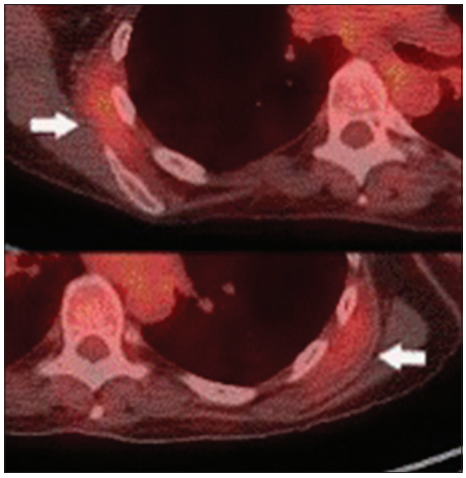

Figure 23: Composite positron emission tomography/computed tomography images of bilateral hypermetabolic elastofibroma dorsi at the postero-lateral aspect of the chest wall (right side: top image, left side: bottom image) located between the ribs and inferior aspect of the scapula (arrows)

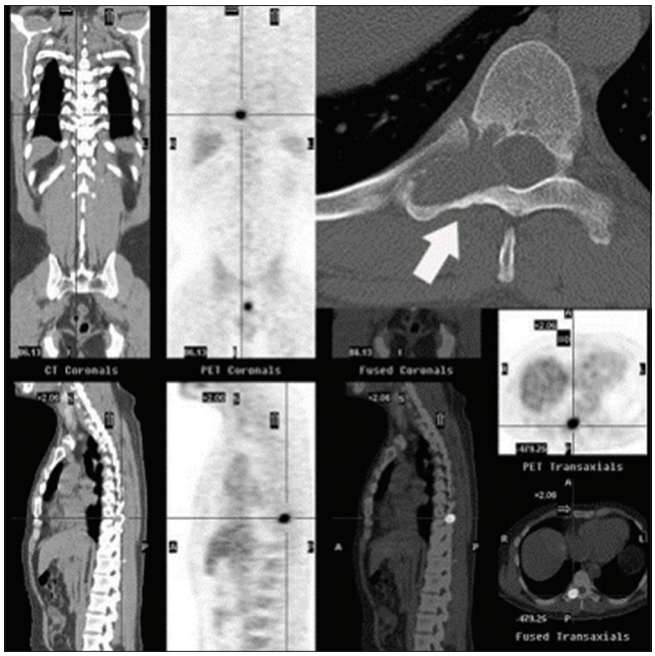

Figure 24: Composite positron emission tomography/computed tomography and computed tomography (upper right corner, arrow) images of an aneurysmal bone cyst of the right aspect of T9 with increased tracer uptake (crosshair)

benign bones tumors may be ^{18}F-FDG avid. They include osteoblastoma, chondromyxoid fibroma, aneurysmal bone cyst [Figure 24], giant cell and brown tumor.[33,34] These lesions cannot be distinguished from malignant bone tumors based on SUV and additional imaging methods (MRI, CT, and radiograph) and ultimately tissue sampling may be required for further characterization.[35]

CONCLUSION

Significant overlap regarding the appearance of inflammatory, infectious and malignant processes exists causing a potential problem in accurate PET/CT interpretation. Benign processes are more inclined to exhibit symmetrical, curvilinear, geometric, anatomic and diffuse scintigraphic features. Malignant lesions usually show a random distribution with nodular, mass-like and amorphous PET/CT features. Correlation with clinical, radiation and surgical history and also imaging cross-check evaluation of contemporary CT, MR and radiographs for the anatomic location and further imaging remains the mainstay of PET/CT characterization of positive findings. For indeterminate cases, tissue sampling remains the only option to adequately identify these indeterminate lesions. Familiarity of false positive findings improves the PET/CT evaluation accuracy of benign lesions of the thorax.

Declaration of patient consent

The authors certify that they have obtained all appropriate patient consent forms. In the form, the patients have given their consent for their images and other clinical information to be reported in the journal. The patients understand that their names and initials will not be published and due efforts will be made to conceal their identity, but anonymity cannot be guaranteed.

Financial support and sponsorship

Nil.

Conflicts of interest

There are no conflicts of interest.

REFERENCES

1. Truong MT, Pan T, Erasmus JJ. Pitfalls in integrated CT-PET of the thorax: Implications in oncologic imaging. J Thorac Imaging 2006;21:111-22.
2. Chang JM, Lee HJ, Goo JM, Lee HY, Lee JJ, Chung JK, *et al*. False positive and false negative FDG-PET scans in various thoracic diseases. Korean J Radiol 2006;7:57-69.
3. Jackson RS, Schlarman TC, Hubble WL, Osman MM. Prevalence and patterns of physiologic muscle uptake detected with whole-body 18F-FDG PET. J Nucl Med Technol 2006;34:29-33.
4. Rosenbaum SJ, Lind T, Antoch G, Bockisch A. False-positive FDG PET uptake-the role of PET/CT. Eur Radiol 2006;16:1054-65.
5. Kavanagh PV, Stevenson AW, Chen MY, Clark PB. Nonneoplastic diseases in the chest showing increased activity on FDG PET. AJR Am J Roentgenol 2004;183:1133-41.
6. Cronin CG, Prakash P, Daniels GH, Boland GW, Kalra MK, Halpern EF, *et al*. Brown fat at PET/CT: Correlation with patient characteristics. Radiology 2012;263:836-42.
7. Maurer AH, Burshteyn M, Adler LP, Steiner RM. How to differentiate benign versus malignant cardiac and paracardiac 18F FDG uptake at oncologic PET/CT. Radiographics 2011;31:1287-305.
8. Franceschi AM, Matthews R, Mankes S, Safaie E, Franceschi D. Four chamber FDG uptake in the heart: An indirect sign of pulmonary embolism. Clin Nucl Med 2012;37:687-91.
9. Lobert P, Brown RK, Dvorak RA, Corbett JR, Kazerooni EA, Wong KK. Spectrum of physiological and pathological cardiac and pericardial uptake of FDG in oncology PET-CT. Clin Radiol 2013;68:e59-71.
10. Kuester LB, Fischman AJ, Fan CM, Halpern EF, Aquino SL. Lipomatous hypertrophy of the interatrial septum: Prevalence and features on fusion 18F fluorodeoxyglucose positron emission tomography/CT. Chest 2005;128:3888-93.
11. Fukuchi K, Ohta H, Matsumura K, Ishida Y. Benign variations and incidental abnormalities of myocardial FDG uptake in the fasting state as encountered during routine oncology positron emission tomography studies. Br J Radiol 2007;80:3-11.
12. Kim JH, Cho JH, Park MS, Chung JH, Lee JG, Kim YS, *et al*. Pulmonary inflammatory pseudotumor-a report of 28 cases. Korean J Intern Med 2002;17:252-8.
13. Alongi F, Bolognesi A, Samanes Gajate AM, Motta M, Landoni C, Berardi G, *et al*. Inflammatory pseudotumor of mediastinum treated with tomotherapy and monitored with FDG-PET/CT: Case report and literature review. Tumori 2010;96:322-6.
14. Kitada M, Matuda Y, Hayashi S, Ishibashi K, Oikawa K, Miyokawa N, *et al*. IgG4-related lung disease showing high standardized uptake values on FDG-PET: Report of two cases. J Cardiothorac Surg 2013;8:160.
15. Gotway MB, Storto ML, Golden JA, Reddy GP, Webb WR.

Incidental detection of thoracic sarcoidosis on whole-body 18fluorine-2- fluoro-2-deoxy-D-glucose positron emission tomography. J Thorac Imaging 2000;15:201-4.
16. Basu S, Saboury B, Werner T, Alavi A. Clinical utility of FDG-PET and PET/CT in non-malignant thoracic disorders. Mol Imaging Biol 2011;13:1051-60.
17. Reichert M, Bensadoun ES. PET imaging in patients with coal workers pneumoconiosis and suspected malignancy. J Thorac Oncol 2009;4:649-51.
18. Saydam O, Gokce M, Kilicgun A, Tanriverdi O. Accuracy of positron emission tomography in mediastinal node assessment in coal workers with lung cancer. Med Oncol 2012;29:589-94.
19. Nakadate M, Yoshida K, Ishii A, Koizumi M, Tochigi N, Suzuki Y, *et al*. Is 18F-FDG PET/CT useful for distinguishing between primary thyroid lymphoma and chronic thyroiditis? Clin Nucl Med 2013;38:709-14.
20. Bakheet SM, Saleem M, Powe J, Al-Amro A, Larsson SG, Mahassin Z. F-18 fluorodeoxyglucose chest uptake in lung inflammation and infection. Clin Nucl Med 2000;25:273-8.
21. Goo JM, Im JG, Do KH, Yeo JS, Seo JB, Kim HY, *et al*. Pulmonary tuberculoma evaluated by means of FDG PET: Findings in 10 cases. Radiology 2000;216:117-21.
22. Kapucu LO, Meltzer CC, Townsend DW, Keenan RJ, Luketich JD. Fluorine-18-fluorodeoxyglucose uptake in pneumonia. J Nucl Med 1998;39:1267-9.
23. Aznar MC, Korreman SS, Pedersen AN, Persson GF, Josipovic M, Specht L. Evaluation of dose to cardiac structures during breast irradiation. Br J Radiol 2011;84:743-6.
24. Prosnitz RG, Hubbs JL, Evans ES, Zhou SM, Yu X, Blazing MA, *et al*. Prospective assessment of radiotherapy-associated cardiac toxicity in breast cancer patients: Analysis of data 3 to 6 years after treatment. Cancer 2007;110:1840-50.
25. Asad S, Aquino SL, Piyavisetpat N, Fischman AJ. False-positive FDG positron emission tomography uptake in nonmalignant chest abnormalities. AJR Am J Roentgenol 2004;182:983-9.
26. Schreiter N, Nogami M, Buchert R, Froeling V, Brenner W, Diekmann F. Pulmonary FDG uptake without a CT counterpart-a pitfall in interpreting PET/CT images. Acta Radiol 2011;52:513-5.
27. Culverwell AD, Scarsbrook AF, Chowdhury FU. False-positive uptake on 2-[^{18}F]-fluoro-2-deoxy-D-glucose (FDG) positron-emission tomography/computed tomography (PET/CT) in oncological imaging. Clin Radiol 2011;66:366-82.
28. Bredella MA, Essary B, Torriani M, Ouellette HA, Palmer WE. Use of FDG-PET in differentiating benign from malignant compression fractures. Skeletal Radiol 2008;37:405-13.
29. Beaulieu S, Rubin B, Djang D, Conrad E, Turcotte E, Eary JF. Positron emission tomography of schwannomas: Emphasizing its potential in preoperative planning. AJR Am J Roentgenol 2004;182:971-4.
30. Hamada K, Ueda T, Higuchi I, Inoue A, Tamai N, Myoi A, *et al*. Peripheral nerve schwannoma: Two cases exhibiting increased FDG uptake in early and delayed PET imaging. Skeletal Radiol 2005;34:52-7.
31. Basu S, Nair N, Banavali S. Uptake characteristics of fluorodeoxyglucose (FDG) in deep fibromatosis and abdominal desmoids: Potential clinical role of FDG-PET in the management. Br J Radiol 2007;80:750-6.
32. Ochsner JE, Sewall SA, Brooks GN, Agni R. Best cases from the AFIP: Elastofibroma dorsi. Radiographics 2006;26:1873-6.
33. Aoki J, Watanabe H, Shinozaki T, Takagishi K, Ishijima H, Oya N, *et al*. FDG PET of primary benign and malignant bone tumors: Standardized uptake value in 52 lesions. Radiology 2001;219:774-7.
34. Costelloe CM, Murphy WA Jr, Chasen BA. Musculoskeletal pitfalls in 18F-FDG PET/CT: Pictorial review. AJR Am J Roentgenol 2009;193:WS1-13, Quiz S26-30.
35. Alavi A, Gupta N, Alberini JL, Hickeson M, Adam LE, Bhargava P, *et al*. Positron emission tomography imaging in nonmalignant thoracic disorders. Semin Nucl Med 2002;32:293-321.